

# 1 **Role of time-averaging of eddy covariance fluxes on water use efficiency** 2 **dynamics of Maize crop**

3 Arun Rao Karimindla, Shweta Kumari, Saipriya SR, Syam Chintala\*, and BVN Phanindra  
4 Kambhammettu

5 Department of Civil Engineering, Indian Institute of Technology Hyderabad, Telangana, India.

6 \*Corresponding author: E-Mail: ce22resch11012@iith.ac.in; Tel: +91 7997014429

## 7 **Abstract**

8 Direct measurement of carbon and water fluxes at high frequency makes eddy  
9 covariance (EC) as the most preferred technique to characterize water use efficiency (WUE).  
10 However, reliability of EC fluxes is largely hinged on energy balance ratio (EBR) and inclusion  
11 of low-frequency fluxes. This study is aimed at investigating the role of averaging period to  
12 represent EC fluxes and its propagation into WUE dynamics. Carbon and water fluxes were  
13 monitored in a drip-irrigated Maize field at 10 Hz frequency and are averaged over 1, 5, 10,  
14 15, 30, 45, 60, and 120 minutes considering daytime unstable conditions. Optimal averaging  
15 period to simulate WUE fluxes for each growth stage is obtained by considering cumulative  
16 frequency (Ogive) curves. A clear departure of EBR from unity was observed during dough  
17 and maturity stages of the crop due to ignorance of canopy heat storage, **low frequency flux**  
18 **losses and inadequate averaging period**. Deviation in representing water (carbon) fluxes  
19 relative to the conventional 30 min average is within  $\pm 3\%$  ( $\pm 10\%$ ) for 10-120 min averaging  
20 and is beyond  $\pm 3\%$  ( $\pm 10\%$ ) for other time-averages. Ogive plots conclude that optimal  
21 averaging period to represent carbon, water and WUE fluxes is 15-30 min for 6<sup>th</sup> leaf and  
22 silking stages, and is 45-60 min for dough and maturity stages. Dynamics of WUE considering  
23 optimal averaging periods are in the range of  $(\mu \pm \sigma)$ : ~~of~~  $1.49 \pm 0.95$ ,  $1.37 \pm 0.74$ ,  $1.39 \pm 0.79$ ,  
24 and  $3.06 \pm 0.69 \mu\text{mol mmol}^{-1}$  for the 6<sup>th</sup> leaf, silking, dough, and maturity stages respectively.  
25 Error in representing WUE with conventional 30 min averaging is marginal ( $< 1.5\%$ )  
26 throughout the crop period except for the dough stage (12.12%). We conclude that the  
27 conventional 30 min averaging of EC fluxes is not appropriate for **the entire growth stage**  
28 **representing WUE throughout the crop period**. Our findings can help in developing efficient  
29 water management strategies by accurately characterizing WUE fluxes from the EC  
30 measurements.

31 **Keywords:** Eddy covariance, Maize crop, Time-average, Energy balance ratio, Ogive  
32 function, Water use efficiency.

33 **Research Highlights:**

- 34 1. The time-averages that yield ~~the~~ most effective energy balance closure are identified as  
35 45 and 60 minutes.
- 36 2. Insufficiently short time-averages such as 1 and 5 minutes, as well as excessively long-  
37 time-averages such as 120 minutes, resulted in a high relative error in representing  
38 carbon and water fluxes.
- 39 3. The conventional 30-minute averaging period proved to be insufficient in capturing  
40 low-frequency fluxes, necessitating the use of longer averaging periods.
- 41 4. Different time averaging periods are to be considered to compute the EC fluxes  
42 considering the crop growth stage.

43 **1.0 INTRODUCTION**

44 Water use efficiency (WUE) is an important eco-hydrologic trait relating two important  
45 processes of plant metabolism namely carbon fixation (via photosynthesis) and water  
46 consumption (via transpiration) (Bramley, 2013). The need for achieving food security with  
47 diminishing water resources under changing climate has made WUE as the controlling  
48 parameter in planning and design of irrigation strategies (Tang, 2015). Depending on the scale  
49 of investigation, WUE can be quantified at: i) leaf, ii) plant, iii) ecosystem, or iv) regional  
50 scales (Medrano, 2015). Of these, ecosystem WUE has taken precedence in irrigation and  
51 agronomy due to: i) accurate and reliable measurement using micrometeorological techniques,  
52 ii) ability to evaluate the role of various water conservation techniques on ecosystem  
53 productivity, and iii) understand the relation between carbon and water cycles in response to  
54 changes in climate (Tang, 2015; Tong, 2014).

55 Eddy covariance (EC) is a non-destructive, micrometeorological technique for direct  
56 measurement of water vapour (H<sub>2</sub>O) and carbon (CO<sub>2</sub>) fluxes between vegetation and  
57 atmosphere at high temporal frequency (Aubinet, 1999; Leclerc and Foken, 2014). EC method  
58 precisely measures the overall transfer of heat, mass, and momentum between the earth's  
59 surface (such as vegetation) and the atmosphere. This is achieved by estimating the covariance  
60 of turbulent fluctuations in vertical wind (referred to as eddies) with respect to the specific flux  
61 under consideration such as H<sub>2</sub>O, CO<sub>2</sub>, temperature. EC represents the scalar fluxes of interest

62 (representative of eco-hydrological processes) from a region upwind of the measurement  
63 known as the footprint. At ecosystem scale, WUE is estimated as the ratio of net primary  
64 product (NPP: proxy for photosynthesis) to evapotranspiration (ET: proxy for water  
65 consumption) (Peddinti, 2020). WUE is a key eco-hydrologic trait that is used to analyse the  
66 role of climate change, drought, deficit irrigation, and management strategies on ecosystem  
67 productivity. Currently, EC is the most accurate and reliable method for estimating carbon and  
68 water exchanges, hence WUE at ecosystem scale (Tong, 2009). A number of studies have  
69 demonstrated the efficacy of EC in estimating WUE across a wide range of ecosystems (Tang,  
70 2015; Tong, 2014; Wang, 2017). Error sources that affect the accuracy of EC fluxes are  
71 grouped into: i) Unrepresentative (due to footprint heterogeneity, unsatisfied underlying  
72 theory), ii) Measurement uncertainties (due to random errors, interference and contamination,  
73 sensor drifts) and iii) Measurement biases in fluxes (tilt, frequency losses, air density  
74 fluctuations etc). Despite improvements in measurement accuracy, data sampling, and  
75 processing techniques, EC method still suffers from the drawback of lack of conservation  
76 among the energy terms, resulting in energy balance closure (EBC) problem (Charuchittipan,  
77 2014; Foken, 2011; Reed, 2018). Lack of EBC as observed in EC system is reported across  
78 diverse ecosystems ranging from simple bare soils (Oncley, 2007), to homogeneous grasslands  
79 (Twine, 2000), to heterogeneous croplands (Peddinti, 2020), to complex forest ecosystem  
80 (Charuchittipan, 2014; Wilson, 2002). Apart from the errors associated with instrumentation,  
81 measurement, and neglected energy sinks, lack of EBC at the EC sites is also attributed to the  
82 omission of low frequency secondary circulations in the turbulent flux estimation (Wilson,  
83 2002). This problem can be circumvented by choosing appropriate averaging period during  
84 flux estimation, the selection of which is based on: i) 'ensemble block time-averaging method'  
85 (Finnigan, 2003; Malhi, 2004; Sakai, 2001), and ii) 'Ogive method' (Berger, 2001).

86 A number of studies have highlighted the importance of averaging period in quantifying  
87 the EC fluxes, with an objective to obtain optimal time-averaging period under various canopy  
88 and surface roughness conditions. While smaller averaging periods (15-30 min) are suitable  
89 for managed croplands, flux estimation from forest and tall canopies demand longer averaging  
90 periods (60-120 min) due to the presence of large-sized, slow moving eddies (Finnigan, 2003;  
91 Sakai, 2001; Sun, 2006). Zhang (2013) concluded that time-averaging of EC fluxes has to be  
92 done in accordance with the observation scale. In an analysis of Chengliu riparian forest in  
93 China, they found that lower time-averaging periods (15 min) are suitable for daily variation  
94 of EC fluxes, whereas higher time-averaging periods (60 min) are suitable for long-term flux

95 computations. A similar observation was made by Lee (2004) over farmlands. In a wheat field  
96 in Yucheng, China, 10 min and 30 min averaging periods were found suitable for diurnal and  
97 long-term flux observations respectively. Flux observations over a Maize crop at Daxing  
98 experimental station in China conclude that optimal time-averaging period has to be considered  
99 in accordance with crop growth stage (Feng, 2017). However, they observed a marginal (< 3  
100 %) error in representing the fluxes at conventional 30 min averaging relative to the optimal  
101 averaging obtained for each growth stage.

102 Maize is the third most important cereal crop in India after rice and wheat, and accounts  
103 for about 10 % of total food production in the country (Sharma, 2018; Ficci 2014). In spite of a  
104 huge area under cultivation (9.4 MHa), high production (23 million tons), and enormous water  
105 consumption (18 BCM), both crop productivity (2.5 t ha<sup>-1</sup>) and crop water productivity (CWP)  
106 (1.83 kg m<sup>-3</sup>) of Indian Maize are far lower than corresponding world averages (Sharma, 2018).  
107 Low CWP (hence, WUE) of Indian Maize can be attributed to: i) a high dependence (85 %) on  
108 erratic, uncertain rainfall, ii) low adoption of hybrid varieties, iii) improper drainage facilities  
109 leading to water logging, and iv) unscientific application of irrigation water without analysing  
110 soil-water-crop interactions (Shankar, 2012). Thus, an accurate quantification of WUE and its  
111 temporal variation during the crop cycle is essential for effective irrigation water management  
112 of Maize crop (Medrano, 2015).

113 While the effect of time-averaging on carbon and water fluxes measured at EC sites is  
114 reported, the effect on their interaction term, i.e. WUE, which is crucial in irrigation water  
115 management is unexplored. Evaluation of time-averaging period on WUE dynamics is  
116 necessary to understand the contribution of low and high frequency photosynthetic carbon and  
117 evaporative water fluxes generated from various field management strategies. Also, most of  
118 the EC flux studies are confined to data rich AmeriFLUX, EuroFLUX, and ChinaFLUX sites,  
119 with limited focus to Indian fragmented croplands. This motivates the present study, and the  
120 objectives of this study are as follows: i) investigate the role of time-averaging of EC fluxes on  
121 EBR and WUE dynamics, ii) compute optimal averaging period to ~~evaluate~~ simulate carbon  
122 and water (hence, WUE) fluxes of Maize crop, and iii) investigate the association of carbon,  
123 water, and WUE fluxes between multiple averaging periods. Results of this study can help in  
124 designing efficient management strategies using EC datasets in response to changes in WUE  
125 during the crop cycle.

126

## 127 2.0 MATERIALS AND METHODOLOGY

### 128 2.1 Site Description and Instrumentation

129 Controlled Maize plots situated at Professor Jaya Shankar Telangana State Agricultural  
130 University (PJTSAU), Hyderabad, Telangana, India (17°19'17" N, 78°24'35" E, 559 m above  
131 sea level) forms the study area. The region is composed of red gravel to sandy loam soils with  
132 field capacity and wilting point in the ranges of 17.92 - 19.56 % and 8.2 – 9.87% respectively.  
133 As per Koppen-Geiger's classification, the region falls under tropical savanna climate zone  
134 (Aw) characterized by long dry and short wet seasons (Kottek, 2006). Mean annual  
135 precipitation of the region is 900 mm (IMD, 2019) with more than 80% occurring during the  
136 monsoon months (Jun-Sep). Temperatures are high during summer (mean ± standard deviation:  
137  $38.33 \pm 2.12$  °C) and low during winter ( $30 \pm 2.20$  °C) months. Humidity of the region varies  
138 from 35% in summer to 73% in monsoon (CGWB, 2013). Mean seasonal wind speed is in the  
139 range of 1.5 to 2.7 m/s (Peddinti, 2020). Hydro-geologically, the study area forms part of the  
140 Deccan plateau characterized by multiple layers of solidified flood basalt resulting from  
141 volcanic eruptions. Depth to groundwater ranges from 12 m (pre-monsoon) to 6 m (post-  
142 monsoon) (CGWB, 2013).

143 Meteorological parameters and turbulent fluxes were obtained for one crop season, i.e.  
144 26 May to 06 Sep, 2019 using an open path eddy covariance (EC) flux tower. The flux system  
145 is composed of integrated CO<sub>2</sub>/H<sub>2</sub>O open-path gas analyzer and 3D sonic anemometer  
146 (IRGASON-EB-NC, Campbell Sci. Inc., USA) to measure CO<sub>2</sub> and H<sub>2</sub>O concentrations at 3  
147 m above the canopy. Raw data was collected with a logger (CR1000, Campbell Sci. Inc., USA)  
148 at 10 Hz frequency. Additionally, slow response meteorological variables including  
149 precipitation (TE525-L-PTL, Tipping Bucket, Campbell Sci. Inc., USA), soil heat flux  
150 (HFP01SC-L-PTL, Campbell Sci. Inc., USA), solar radiation (CNR 4, Campbell Sci. Inc.,  
151 USA), and soil moisture (CS616-L-PT-L, Campbell Sci. Inc., USA) were obtained at 10 min  
152 intervals.

153

### 154 2.2 Data Collection and Processing

155 Table 1 shows the phenological stages of the Maize crop in the study area (Soujanya,  
156 2021). Additionally, leaf-area index (LAI) and mean plant height were monitored during the  
157 crop cycle (Table 1). The LAI was measured using the plant canopy analyser, whereas the plant

158 height was measured using a ruler from the base of the plant to its crown. Maize crops of the  
 159 experimental fields are sown on 25<sup>th</sup> May 2019 and harvested on 6<sup>th</sup> September 2019 with a  
 160 base period of 104 days.

161 **Table 1:** Phenological growth stages and physical properties of the Maize crop

S. No.	Growth stage	Start date	End date	Period Length (days)	Leaf Area Index (m <sup>2</sup> m <sup>-2</sup> )	Plant height (cm)
1	6 <sup>th</sup> leaf	26/05/2019	12/06/2019	18	0.61	46.8
2	Silking	13/06/2019	19/07/2019	37	1.56	75.2
3	Dough	20/07/2019	12/08/2019	24	3.46	133
4	Maturity	13/08/2019	06/09/2019	25	3.03	134

162

163 Data from the EC system at 10 Hz frequency was converted to ASCII format using  
 164 LoggerNet (4.3) software (Campbell Scientific Inc., Logan, Utah, USA), and further  
 165 aggregated to various averaging periods (1, 5, 10, 15, 30, 45, 60, and 120 minutes). Post data  
 166 processing was done using EddyPro post-processing software (version 7.0.8, LI-COR, USA).  
 167 Primary corrections performed on the raw dataset include tilt corrections, turbulent  
 168 fluctuations, density fluctuations, frequency corrections and quality checks. Tilt corrections  
 169 were made by the double axis rotation method for each averaging period. Either block average  
 170 method or linear trending method were considered to compute the turbulent fluctuations. Block  
 171 averaging method was used for detrending the fluxes at 1, 5, 10, 30, 45, and 60 min averaging  
 172 periods. Longer averaging periods (e.g. 120 min) has resulted in inconsistency in the obtained  
 173 fluxes, which is a weakness of the block averaging (Renhua, 2005; Sun et al., 2006) . Hence,  
 174 linear trend removal method was used to compute the fluxes for 120 min averaging period.  
 175 Density fluctuation corrections were done using Webb–Pearman–Leuning (WPL)  
 176 method. Quality checks were performed following a flagging policy proposed by Mauder and  
 177 Foken (2006) (0-1-2 system). Flag set to "0" corresponds to the best quality fluxes, "1"  
 178 corresponds to fluxes acceptable for general analysis, and "2" corresponds to poor quality  
 179 fluxes that should be removed from the dataset. The resulting fluxes may exhibit spikes,

180 discontinuity, randomness etc. There is a need to perform secondary corrections on the data  
 181 that include flux spike removal (Vickers and Mahrt 1997), friction velocity corrections (to filter  
 182 night time observations), gap filling and uncertainty analysis (Finkelstein, 2001), skewness &  
 183 kurtosis removal, spectral corrections, and frequency corrections. To correct flux estimates for  
 184 low and high frequency losses due to instrument setup, intrinsic sampling limits of the devices,  
 185 and various data processing decisions, spectral corrections are performed. Additionally, slow  
 186 sensor meteorological data obtained at 1 min interval were processed for different time-  
 187 averaging periods using the EddyPro post-processing software (version 7.0.8, LI-COR, USA).

188

### 189 **2.3 Effect of time-averaging on EBR and EC fluxes**

190 Violation of law of conservation of energy resulting from the EC observed energy terms  
 191 is referred as energy balance closure (EBC). The available energy ( $R_n-G$ ) is generally higher  
 192 than the turbulent fluxes ( $H+LE$ ), resulting in a positive balance (Eshonkulov, 2019) where  $R_n$ ,  
 193  $G$ ,  $H$  and  $LE$  correspond to net radiation, soil heat flux, sensible heat and latent heat  
 194 respectively. Apart from instrument and measurement issues, this lack of energy closure is  
 195 thought to be partly from averaging periods and coordinate systems (Finnigan, 2003; Finnigan,  
 196 2004; Gerken, 2018). The energy closure fraction, commonly termed as energy balance ratio  
 197 (EBR) is used to evaluate the quality of EC data by examining energy fluxes at the surface  
 198 (Chen and Li 2012), given by:

$$199 \quad EBR = \frac{H+LE}{R_n-G} \quad (1)$$

$$200 \quad H = \rho_a C_p \overline{w'T'} \quad (2)$$

$$201 \quad LE = L_v \overline{w'\rho_v'} \quad (3)$$

202 where  $\rho_a$  is the air density;  $C_p$  is the specific heat of air,  $w'$  is the wind velocity fluctuation,  $T'$   
 203 is the temperature fluctuation,  $L_v$  is the latent heat of vaporization and  $\rho_v'$  is the H<sub>2</sub>O gas  
 204 concentration fluctuation.

205 EBR helps to determine the averaging period required to calculate H and LE fluxes over a  
 206 range of landscapes (Chen and Li 2012). A high EBR ( $EBR \geq 0.7$ ) ensures reliability of EC  
 207 observations for use with flux estimation (Barr et al., 2006; Kidston et al., 2010).

208 Eddy fluxes are computed as the covariance between instantaneous deviation in vertical  
209 wind speed ( $w'$ ) and scalar component of interest ( $s'$ ) from their respective means, given by

$$210 \quad F \approx \overline{\rho_a w' s'} \quad (4)$$

211 where  $\overline{\rho_a}$  is the mean air density, and the overbar represents the time-average of eddy fluxes,  
212 which is of interest in the present study. Depending on the scalar component considered (ex:  
213 temperature, water vapour (H<sub>2</sub>O), carbon dioxide (CO<sub>2</sub>) concentration), corresponding eddy  
214 fluxes (ex: sensible heat, latent heat, carbon flux) are computed as below.

$$215 \quad F_{CO_2} \approx \overline{\rho_a w' CO_2'} \quad (5)$$

$$216 \quad F_{H_2O} \approx \overline{\rho_a w' H_2O'} \quad (6)$$

217 Ecosystem WUE is then estimated as the ratio of daytime carbon (net primary product) to water  
218 fluxes (evapotranspiration), observed considering daytime unstable atmospheric conditions  
219 (08:00 am to 04:00 pm) given by:

$$220 \quad WUE = \frac{NPP}{ET} = \frac{F_{CO_2}}{F_{H_2O}} \quad (7)$$

221 Fluxes originating from real-world sites are composed of both high frequency (turbulence) and  
222 low frequency (advection) fluctuations, with a spectral gap in between. Isolating local  
223 turbulence component for use with flux studies is achieved by choosing an appropriate  
224 averaging period,  $T_1$  (typically 30 minutes) on fast response measurements operating at high  
225 frequency  $T_2$  (Manon and Kristian 2020). Optimal averaging period ( $T_1$ ) should be long enough  
226 to reduce random error (Berger, 2001) and short enough to avoid non-stationarity associated  
227 with advection (Foken & Wichura, 1996). The flux estimates (eq. 2) are further decomposed  
228 into frequency dependent contributions, known as co-spectra  $Co_{ws}(f)$  between vertical wind  
229 velocity ( $w$ ) and scalar of interest ( $s$ ) for frequencies ' $f$ ' (Manon and Kristian 2020). For an  
230 accurate estimation of the flux, it is essential that the EC method is applied under conditions  
231 where the flow is stationary, and all eddies carrying flux are sampled. Given that the flow  
232 remains stationary, an 'Ogive' serves as a check for the essential requirement to sample all  
233 scales carrying the flux. Ogive function is well proposed to check if all low frequency fluxes  
234 are included in the turbulent flux measured with the EC method (Foken & Wichura, 1996;  
235 Foken et al., 2005). It is used to investigate the energy balance losses caused by low frequency  
236 fluxes. Ogive analysis is performed to investigate the flux contribution from each frequency



237 range and to arrive at most suitable averaging period to capture most of the turbulent fluxes  
 238 (Desjardans, 1989; Charuchittipan, 2014). Ogive function thus provides the cumulative sum of  
 239 co-spectral energy starting from the highest frequency, given by:

$$240 \quad \text{Og}_{\text{ws}}(f_0) = \int_{f_0}^{\infty} \text{Co}_{\text{ws}}(f) df \quad (8)$$

241 The point of convergence on the Ogive plot to an asymptote corresponds to optimal averaging  
 242 period ( $T_1$ ) for use with averaging of high frequency turbulence fluxes. In other words, the  
 243 point at which the Ogive plot flattens out represents the optimal averaging period. A total of  
 244 eight averaging periods, i.e., 1, 5, 10, 15, 30, 45, 60, and 120 minutes were considered to  
 245 investigate the role of time-averaging on EBR, EC and WUE fluxes, and further to arrive at the  
 246 optimum averaging period for use with WUE estimation. The biophysical and physiological  
 247 characteristics such as plant height, crop water requirement, LAI, etc. changes with respect to  
 248 the crop growth stage (Chintala et al., 2024) and have a significant effect on the EC fluxes.  
 249 Since these factors vary over growth stages, time-averaging of EC fluxes is separated based on  
 250 crop growth stage.

251

## 252 **2.4 Performance Evaluation**

253 The ability of various averaging periods to close the energy balance and compute the  
 254 EC fluxes is evaluated using three goodness of fit indicators, namely: a) coefficient of  
 255 determination ( $R^2$ ), b) root mean squared error (RMSE), and c) relative error (RE). While  $R^2$   
 256 and RMSE aim to quantify the error in closing the energy balance, RE is aimed to compute the  
 257 error in estimating EC fluxes with conventional 30 min averaging period relative to optimal  
 258 averaging period.

259 Root mean square error (RMSE) measures overall accuracy in closing the energy balance for  
 260 a given averaging period by penalizing large errors heavily, given by:

$$261 \quad \text{RMSE} = \left[ \frac{\sum_{i=1}^n ((R_n - G_i) - (H + LE)_i)^2}{n} \right]^{0.5} \quad (9)$$

262 where n is the number of observations.

263 Coefficient of determination ( $R^2$ ) and Pearson correlation coefficient (r) are the measures of  
 264 the strength of linear association between turbulent fluxes and available energy, given by:

$$R^2 = \frac{\left( \frac{\sum_{i=1}^n [(R_n - G)_i - \overline{(R_n - G)}] [(H + LE)_i - \overline{(H + LE)}]}{\sqrt{\sum_{i=1}^n [(R_n - G)_i - \overline{(R_n - G)}]^2 [(H + LE)_i - \overline{(H + LE)}]^2}} \right)^2}{\left( \frac{\sum_{i=1}^n [(R_n - G)_i - \overline{(R_n - G)}] [(H + LE)_i - \overline{(H + LE)}]}{\sqrt{\sum_{i=1}^n [(R_n - G)_i - \overline{(R_n - G)}]^2 [(H + LE)_i - \overline{(H + LE)}]^2}} \right)^2} \quad (10)$$

$$R^2 = \left\{ \frac{\sum_{i=1}^n [(R_n - G)_i - \overline{(R_n - G)}] [(H + LE)_i - \overline{(H + LE)}]}{\sqrt{\sum_{i=1}^n [(R_n - G)_i - \overline{(R_n - G)}]^2 [(H + LE)_i - \overline{(H + LE)}]^2}} \right\}^2$$

$$r = \left\{ \frac{\sum_{i=1}^n [(R_n - G)_i - \overline{(R_n - G)}] [(H + LE)_i - \overline{(H + LE)}]}{\sqrt{\sum_{i=1}^n [(R_n - G)_i - \overline{(R_n - G)}]^2 [(H + LE)_i - \overline{(H + LE)}]^2}} \right\} \quad (11)$$

268 Relative error (RE) provides the disparity in the fluxes estimated with conventional (30 min)  
269 relative to the fluxes estimated with optimal averaging period, given by:

$$RE = \left[ \frac{F_{opt} - F_{30min}}{F_{opt}} \right] \times 100 \quad (12)$$

271 where  $F_{opt}$  and  $F_{30}$  are the flux of interest considering optimal and conventional (30 min)  
272 averaging periods.

273 Averaging period corresponding to high  $R^2$  (close to 1), low RMSE (close to zero) is considered  
274 to be the optimal choice in representing the EC fluxes.

275

### 276 3.0 RESULTS AND DISCUSSION

#### 277 3.1 Diurnal variations in energy balance components

278 To understand the energy variation in response to rapid changes in meteorological  
279 conditions, we analysed the diurnal variations in energy balance components. Figure 1 shows

Formatted: Font: 10 pt, Not Highlight

Formatted: Font: 10 pt, Not Highlight

Formatted: Font: 10 pt, Not Highlight

Formatted: Font: 10 pt, Not Highlight

Formatted: Font: 10 pt, Not Highlight

Formatted: Font: 10 pt, Not Highlight

Formatted: Font: 10 pt, Not Highlight

Formatted: Font: 10 pt, Not Highlight

Formatted: Font: 10 pt, Not Highlight

Formatted: Font: 10 pt, Not Highlight

Formatted: Font: 10 pt, Not Highlight

Formatted: Font: 10 pt, Not Highlight

Formatted: Font: 10 pt, Not Highlight

Formatted: Font: 10 pt, Not Highlight

Formatted: Font: 10 pt, Not Highlight

Formatted: Font: 10 pt, Not Highlight

Formatted: Font: 10 pt, Not Highlight

Formatted: Font: 10 pt, Not Highlight

Formatted: Font: 10 pt, Not Highlight

Formatted: Font: 10 pt, Not Highlight

Formatted: Font: 10 pt, Not Highlight

Formatted: Font: 10 pt, Not Highlight

Formatted: Font: 10 pt, Not Highlight

Formatted: Font: 10 pt, Not Highlight

Formatted: Font: 10 pt, Not Highlight

Formatted: Font: 10 pt, Not Highlight

Formatted: Font: 10 pt, Not Highlight

Formatted: Font: 10 pt, Not Highlight

Formatted: Font: 10 pt, Not Highlight

Formatted: Font: 10 pt, Not Highlight

Formatted: Font: 10 pt, Not Highlight

Formatted: Font: 10 pt, Not Highlight

Formatted: Font: 10 pt, Not Highlight

Formatted: Font: 10 pt, Not Highlight

Formatted: Font: 10 pt, Not Highlight

Formatted: Font: 10 pt, Not Highlight

Formatted: Font: 10 pt, Not Highlight

Formatted: Font: 10 pt, Not Highlight

Formatted: Font: 10 pt, Not Highlight

Formatted: Font: 10 pt, Not Highlight

Formatted: Font: 10 pt, Not Highlight

Formatted: Font: 10 pt, Not Highlight

Formatted: Font: 10 pt, Not Highlight

Formatted: Font: 10 pt, Not Highlight

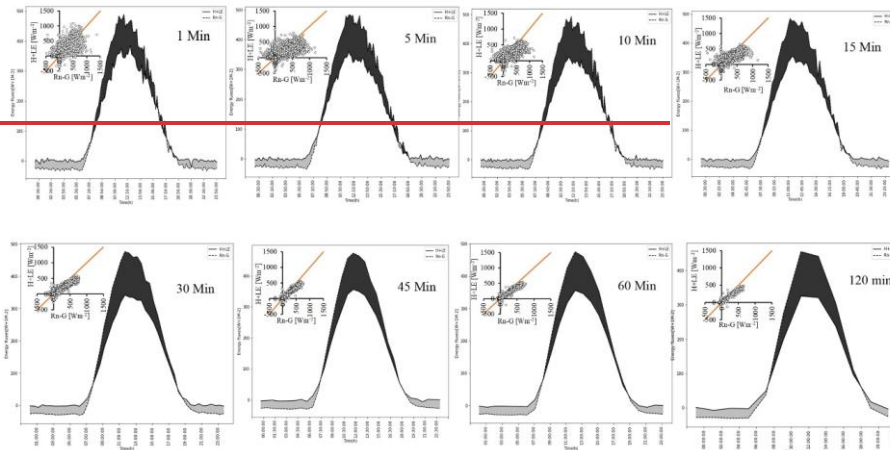
Formatted: Font: 10 pt, Not Highlight

Formatted: Font: 10 pt, Not Highlight

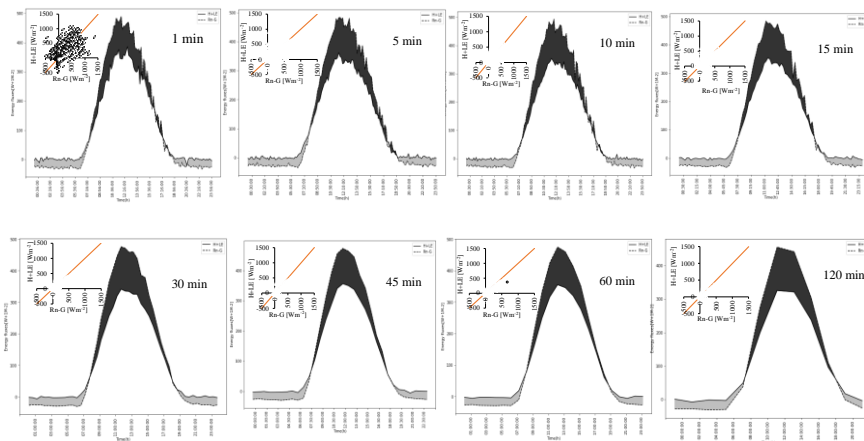
Formatted: Font: 10 pt, Not Highlight

Formatted: Font: 10 pt, Not Highlight

280



281



282 **Figure 1:** Diurnal variations in energy balance components (available energy:  $R_n-G$  and turbulent fluxes:  
 283  $H+LE$ ) during the crop cycle with different averaging periods. Inset: Scatter-plots between the two  
 284 datasets.

285 the diurnal variations in available energy ( $R_n-G$ ) and turbulent fluxes ( $H+LE$ ) averaged over  
 286 the crop cycle for various time-averages. The diurnal variations of ( $R_n-G$ ) and ( $H+LE$ ) are bell-  
 287 shaped, with peak occurring at around noon ( $480.16 \pm 14.15 \text{ Wm}^{-2}$ ,  $356.23 \pm 18.51 \text{ Wm}^{-2}$ )  
 288 (Figure 1). The energy balance difference (shaded areas of the figure) is found to be positive  
 289 ( $76.88 \pm 43.14 \text{ Wm}^{-2}$ ) during daylight hours (08:00 am to 06:00 pm) and is negative ( $-24 \pm$   
 290  $11.65 \text{ Wm}^{-2}$ ) for the remaining time. The vertical offset between the two curves, representing  
 291 the residual of energy balance is highest around the noon ( $142.39 \pm 19.42 \text{ Wm}^{-2}$ ), and is

292 consistent between the averaging periods. For an average site-day, the cumulative energy  
 293 balance difference was found to be constant with a mean of  $1811 \pm 91.56 \text{ Wm}^{-2}$  at all averaging  
 294 periods. The cumulative energy balance difference is crossing the 'zero' line at around 11:30  
 295 am. The variation is rough at lower averaging periods due to a high sample size ( $n= 10859$  at  
 296  $T = 1 \text{ min}$ ) and is gradually smoothed towards higher averaging periods ( $n= 811$  at  $T = 120$   
 297 min). The variation is rough at lower averaging periods due to a high sample size ( $n= 10859$  at  
 298  $T = 1 \text{ min}$ ) and is gradually smoothed towards higher averaging periods ( $n= 811$  at  $T = 120$   
 299 min). The shorter averaging periods has introduced random uncertainty in the datasets during  
 300 coordinate rotation correction. The slope of regression lines between (H+LE) and ( $R_n$ -G)  
 301 considering all averaging periods are in the range of 0.59 to 0.71 with a mean of  $0.65 \pm 0.041$ .  
 302 The intercept is ranged from 19.01 to  $31.56 \text{ Wm}^{-2}$ . The best slope ( $\geq 0.70$ ) and intercept ( $\leq 20$   
 303  $\text{Wm}^{-2}$ ) were achieved with 45 and 60 minutes averaging periods, which is consistent with  
 304 literature (Gao, 2017; Leuning, 2012). This conclude that, longer averaging periods have a  
 305 good closure over shorter averaging periods. The strength of linear association between ( $R_n$ -G)  
 306 and (H+LE) around the best fit line, explained by  $r$  is high ( $0.80 < r \leq 0.9$ ) at low averaging  
 307 periods, i.e., 1, 5, 10 minutes, and is very high ( $r > 0.9$ ) for other averaging periods (Table 2).  
 308 However, the departure of the data from 1:1 line is relatively low both at short and long  
 309 averaging periods. Our findings show that averaging period has minimal influence in  
 310 representing the energy balance terms. However, data scatter around 1:1 line is high for shorter  
 311 time-averages due to large sample size and data randomness.

312 **Table 2:** Summary of linear regression parameters in closing the energy balance with different  
 313 averaging periods.

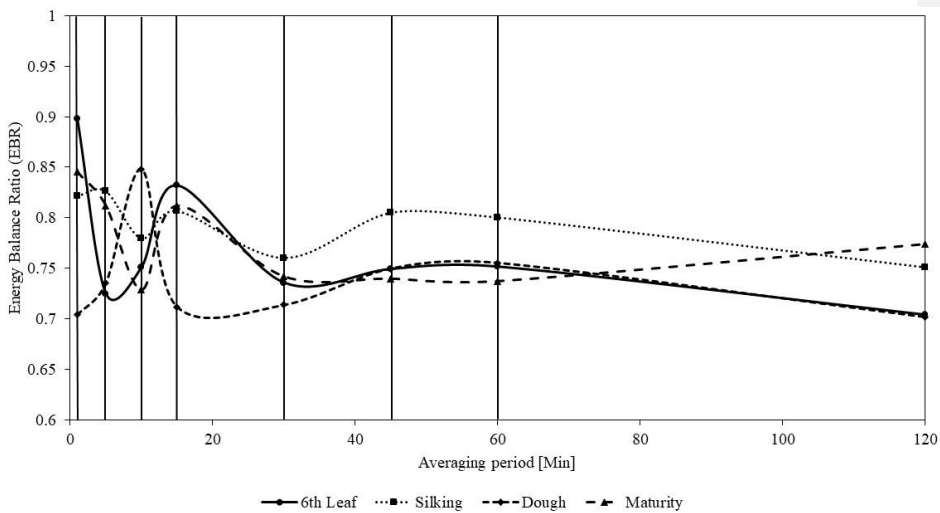
Averaging Period	Slope	R <sup>2</sup>	Intercept (Wm <sup>-2</sup> )	r	N	RMSE (Wm <sup>-2</sup> )
1min	0.63	0.66	30.31	0.81	10859	98.38
5min	0.59	0.74	31.56	0.86	10785	76.47
10min	0.60	0.80	28.94	0.90	10753	64.41
15min	0.63	0.84	26.56	0.92	7150	58.18

30min	0.66	0.93	20.49	0.96	3554	38.33
45min	0.70	0.94	19.99	0.97	2355	36.30
60min	0.71	0.94	19.01	0.97	1765	35.07
120min	0.67	0.93	20.77	0.96	811	39.95

314

315 **3.2 Effect of averaging period on EBR and EC fluxes**

316 The variation in energy balance ratio (EBR) with averaging period for individual  
317 growth stages of the crop is presented in Figure 2. We observed a clear departure of EBR from



318

319 **Figure 2:** Variation in energy balance ratio (EBR) with averaging period for different growth stages. (Solid  
320 verticals from left to right correspond to the averaging periods of 1 min, 5 min, 10 min, 15 min, 30 min, 45  
321 min, 60 min, and 120 min respectively).

322 unity for all growth stages, particularly with dough and maturity stages due to ignorance of  
323 canopy heat storage, [low frequency flux losses and inadequate time averaging period \(Meyers  
324 and Hollinger, 2004; Rahman et al., 2019\)](#). EBR is fluctuating between 0.70 and 0.90 at low (1  
325 – 30 min) averaging periods and is fairly constant ([mean: 0.75 ± 0.03](#)) at high ( $\geq 30$  min)  
326 averaging periods. Our reported values of EBR during the crop growth are within the typically  
327 found range of 0.65 to 1.2 for most of the crops (Feng, 2017; Finnigan, 2003; Wilson, 2002).  
328 The mean EBR with conventional 30 min averaging period is found to be 0.74, 0.76, 0.71, and

Formatted: No Spacing

Formatted: Font: (Default) Times New Roman, 12 pt,  
Font color: Black

329 0.74 during 6<sup>th</sup> leaf, silking, dough, and maturity stages respectively. Low EBR during the crop  
 330 cycle can also be attributed to the ignorance of energy transport associated with large eddies  
 331 from landscape heterogeneity (Meyers and Hollinger, 2004; Rahman et al., 2019). However,  
 332 EC method assumes the landscape within the footprint of measurement to be flat and  
 333 homogenous. ~~This violation might have lowered the EBR. We could not observe any~~  
 334 ~~significant differences in temporal trends of 'wind speed' and 'wind direction' between the~~  
 335 ~~averaging periods, hence meteorological conditions were not analysed by varying time-~~  
 336 ~~average. We did not observe variations in optimal averaging time due to changes in wind speed~~  
 337 ~~and direction, hence meteorological conditions were not analysed in this study.~~ Changes in  
 338 daytime mean carbon and water fluxes with averaging period for different growth stages of the  
 339 crop is shown in Figure 3. Carbon fluxes (sink) have a very low mean ( $1.81 \pm 0.06 \mu\text{mol m}^{-2}\text{s}^{-1}$ )  
 340 during 6<sup>th</sup> leaf stage, low mean during silking ( $3.48 \pm 0.07 \mu\text{mol m}^{-2}\text{s}^{-1}$ ) and dough ( $3.03 \pm$   
 341  $0.87 \mu\text{mol m}^{-2}\text{s}^{-1}$ ) stages, and a high mean ( $15.44 \pm 0.75 \mu\text{mol m}^{-2}\text{s}^{-1}$ ) during maturity stage.

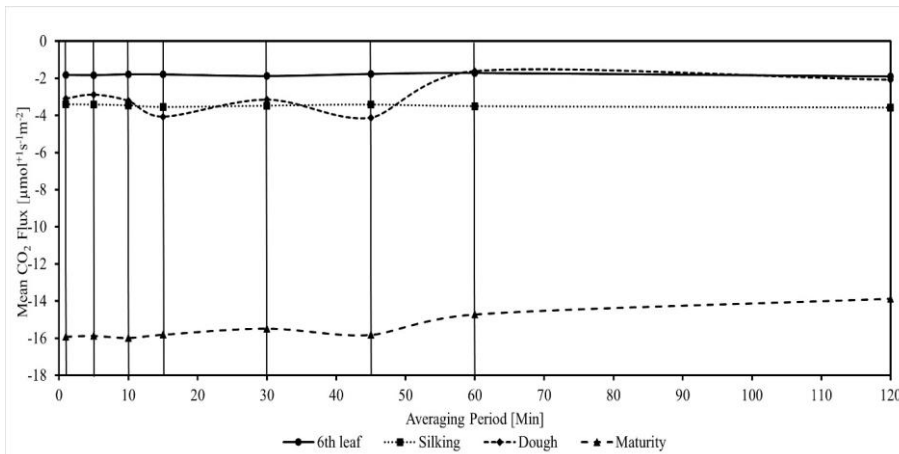
Formatted: Font: (Default) Times New Roman, 12 pt,  
 Font color: Black

Formatted: Not Highlight

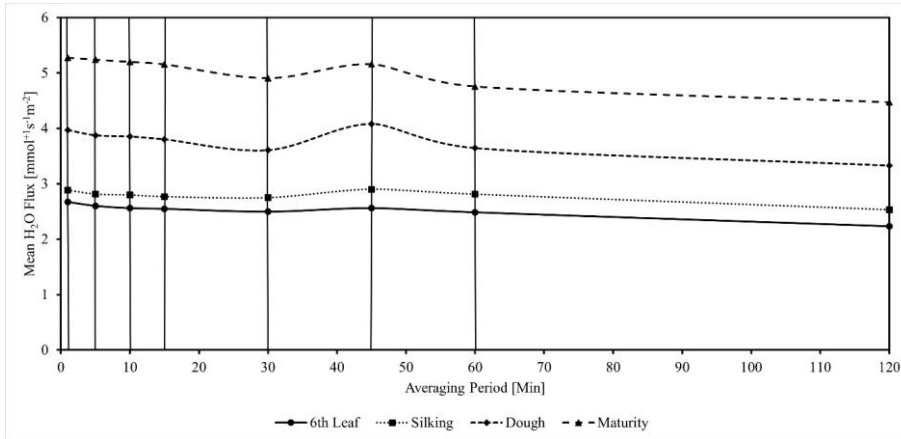
Formatted: Not Highlight

Formatted: Not Highlight

Formatted: Font: Font color: Dark Blue, Highlight



342  
 343 **Figure 3a:** Variation in mean carbon fluxes with averaging period for different growth stages (Solid verticals  
 344 from left to right correspond to the averaging periods of 1 min, 5 min, 10 min, 15 min, 30 min, 45 min, 60  
 345 min, and 120 min respectively).  
 346



347  
348 **Figure 3b:** Variation in mean water fluxes with averaging period for different growth stages (Solid verticals  
349 from left to right correspond to the averaging periods of 1 min, 5 min, 10 min, 15 min, 30 min, 45 min, 60  
350 min, and 120 min respectively).

351 Mean carbon fluxes during 6<sup>th</sup> leaf and silking stage are mostly unaffected by averaging period.

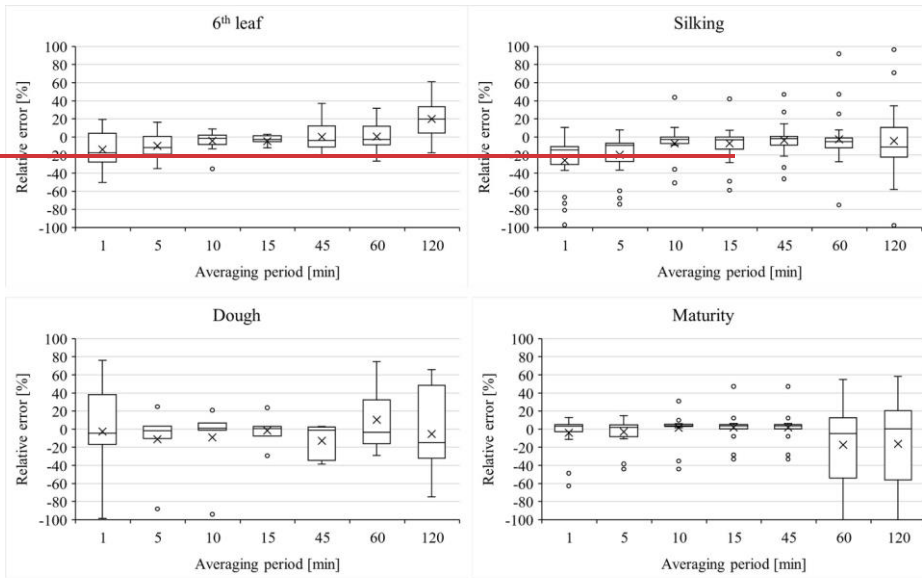
352 We observed a gradual increase in water vapour fluxes during the crop cycle from 6<sup>th</sup> leaf ( $2.52$   
353  $\pm 0.13$   $\text{mmol s}^{-1}\text{m}^{-2}$ ) to maturity ( $5.02 \pm 0.29$   $\text{mmol s}^{-1}\text{m}^{-2}$ ). From the mean  $\text{CO}_2$  and  $\text{H}_2\text{O}$  flux  
354 dynamics, it is observed that the drip irrigated Maize crop is acting as a carbon sink in the entire  
355 crop season especially in the latter stages of the crop i.e. maturity stage with a mean of  $15.44$   
356  $\mu\text{mol m}^{-2}\text{s}^{-1}$ . This is clearly evident from the increasing trend of LAI and plant height during  
357 the crop season. Such an increase is highlighted by previous studies of Guo et al., 2021. At the  
358 same time, mean  $\text{H}_2\text{O}$  fluxes were increased towards the end of crop growing season due to  
359 increased crop water demand. As the averaging period is increased, the mean water vapour flux  
360 is decreased, with an exception at 45 min averaging period. Deviation in representing carbon  
361 and water fluxes at different averaging periods, relative to the conventional 30 min averaging  
362 period i.e. relative error (RE) is presented in Figure 4. The RE is obtained by considering daily  
363 averages in the deviations for each growth stage. During 6<sup>th</sup> leaf and silking stages, RE in  
364 estimating carbon fluxes is high ( $\sim -15\%$ ) with low averaging periods, and is gradually  
365 diminishing towards higher averaging periods, with an exception at very high (120 min)  
366 average period. For dough and maturity stages, RE is found to be significant with higher  
367 averaging periods (60-120 min). RE in estimating water vapour fluxes is found to be  
368 insignificant at all averaging periods for the 6<sup>th</sup> leaf and silking stages. However, dough and  
369 maturity stages have shown a large variation in RE considering either too-short (1, 5 min) or  
370 too-long (60, 120 min) time averages. A high variability variation in RE for time scales larger

Formatted: No Spacing

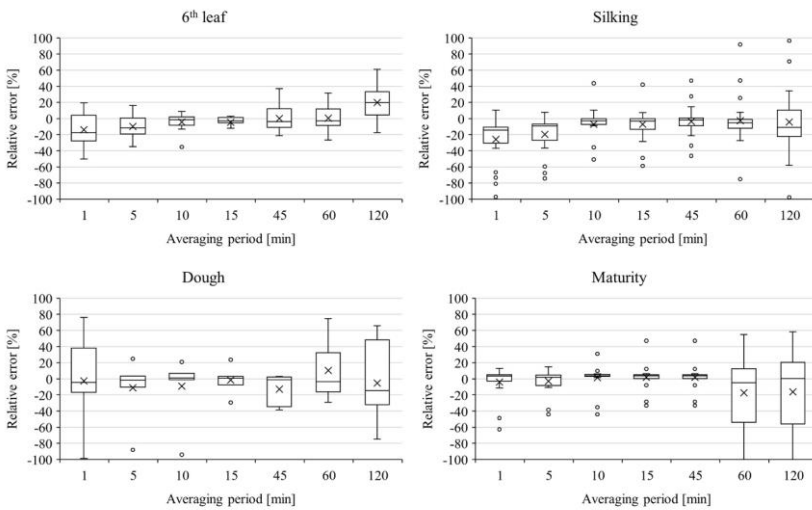
371 than 45 min indicate the effects of sub mesoscale (non-turbulent) motions. Hence, 45 min  
372 average period can be considered as optimal in isolating the turbulence components for use  
373 with flux representation.

Formatted: Font:

374



375

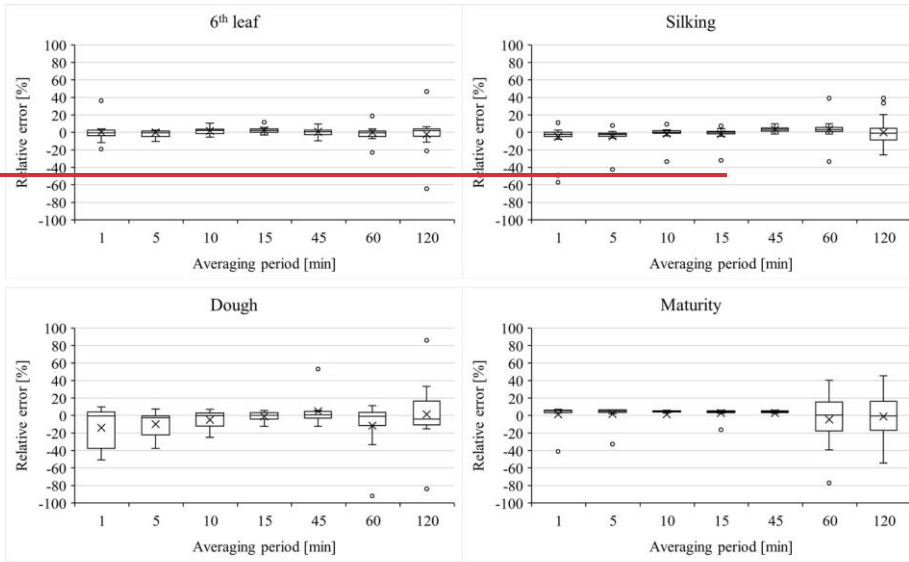


376

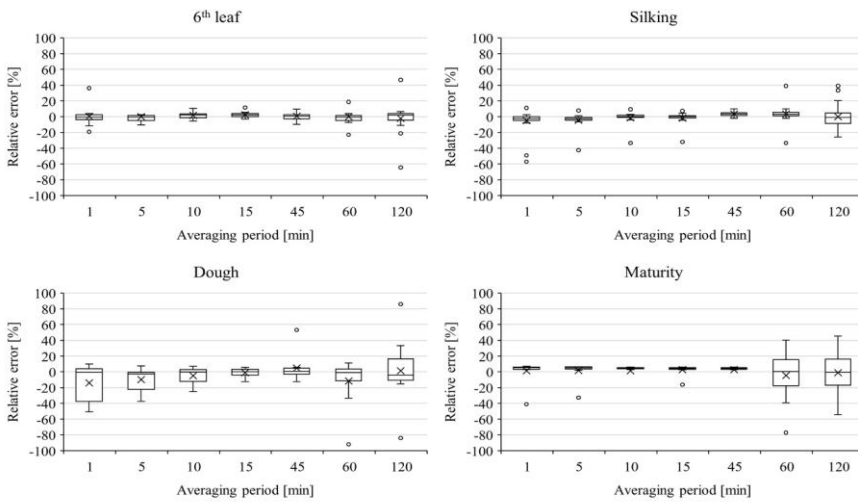
377 **Figure 4a:** Whisker plots showing the distribution of error in estimating carbon fluxes with various  
378 averaging periods relative to the conventional 30 min averaging.



379



380



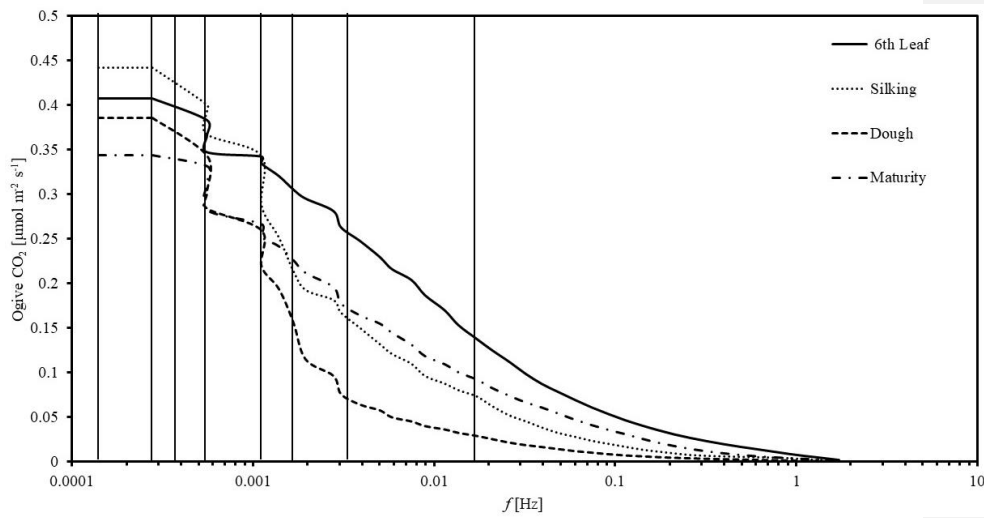
381

382 **Figure 4b:** Whisker plots showing the distribution of error in estimating water fluxes with various averaging  
383 periods relative to the conventional 30 min averaging.

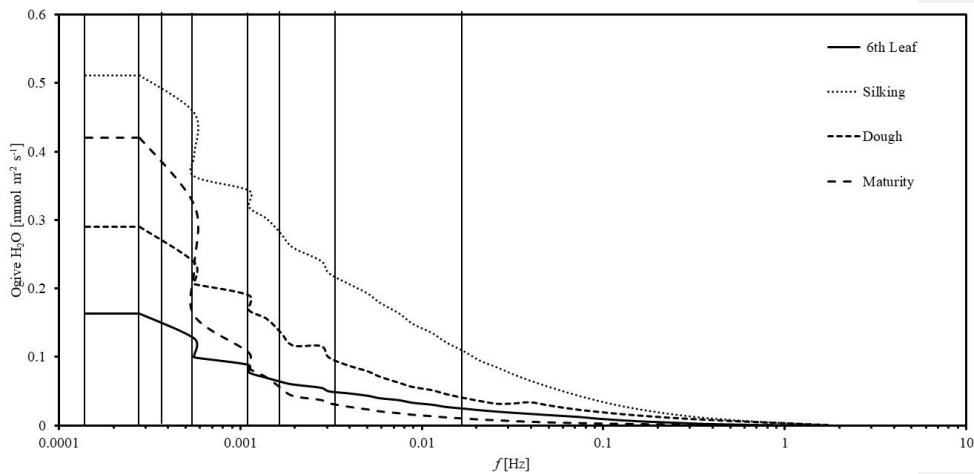
384

385 **3.3 Selection of Optimal averaging period**

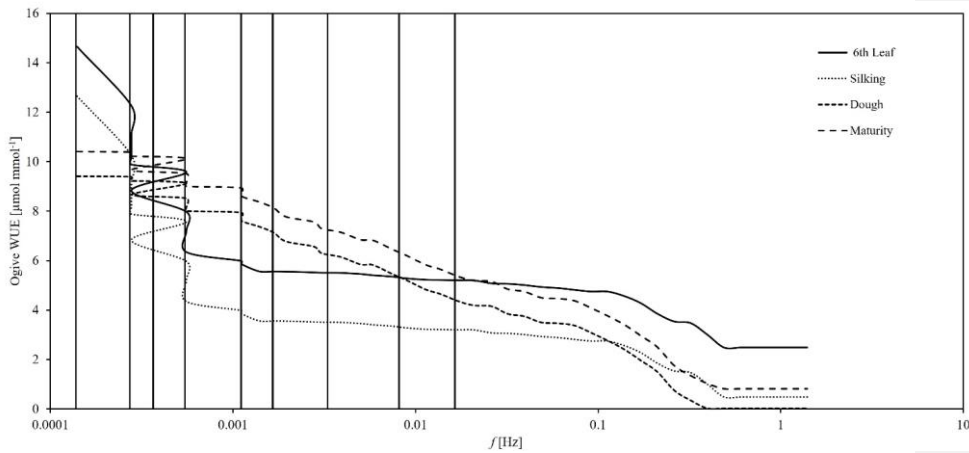
386 Ogive functions representing the cumulative integral of the co-spectral energy starting  
 387 with highest frequency, i.e., 0.016 Hz ( $T = 1$  min) for carbon, water, and WUE fluxes are  
 388 presented



389  
 390 **Figure 5a:** Ogive plots of carbon fluxes for different growth stages of the Maize crop. (Solid verticals from  
 391 left to right extremes correspond to the averaging periods of 120 min, 60 min, 45 min, 30 min, 15 min, 10  
 392 min, 5min and 1 min respectively).



393  
 394 **Figure 5b:** Ogive plots of water fluxes for different growth stages of the Maize crop. (Solid verticals from  
 395 left to right extremes correspond to the averaging periods of 120 min, 60 min, 45 min, 30 min, 15 min, 10  
 396 min, 5min and 1 min respectively)



397

398 **Figure 5c:** Ogive plots of water use efficiency for different growth stages of the Maize crop. (Solid verticals  
 399 from left to right extremes correspond to the averaging periods of 120 min, 60 min, 45 min, 30 min, 15 min,  
 400 10 min, 5min and 1 min respectively)

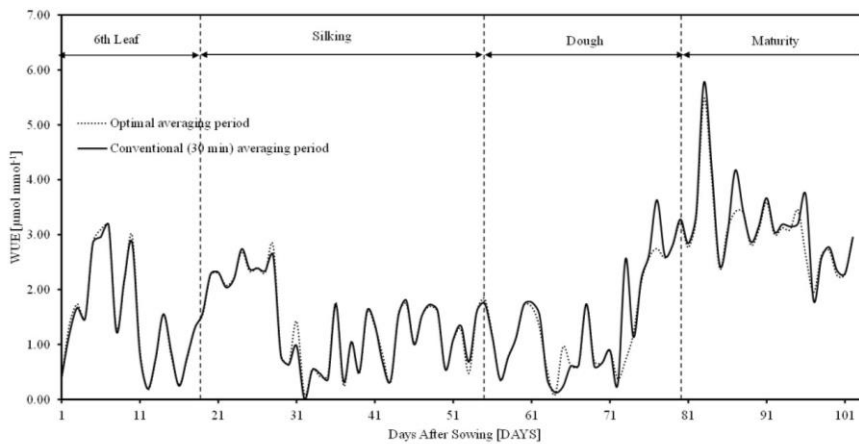
401 in Figure 5. Shorter time periods corresponding to daytime unstable atmospheric conditions  
 402 (08:00 am to 04:00 pm) for various growth stages were investigated. Ogive plots of carbon  
 403 fluxes for 6<sup>th</sup> leaf and silking stages showed an increasing trend up to 0.011 Hz (15 min) and  
 404 remained fairly constant before 0.0055 Hz (30 min). This concludes that whole turbulent  
 405 spectrum can be covered with 15 to 30 min averaging, with negligible flux contribution from  
 406 longer frequencies. Ogive plots of carbon fluxes for dough and maturity stages showed a  
 407 continuous increasing trend without a defined plateau (horizontal asymptote) in between. This  
 408 conclude that the conventional 30 min averaging period is inadequate to capture the low  
 409 frequency fluxes, thus demanding for higher averaging periods. We observed a similar  
 410 behaviour with water fluxes (Figure 5b). The flat part of the Ogive curve representing the  
 411 optimal averaging period was found to vary across the crop cycle. While 15-30 min time-  
 412 average is suitable for aggregating the EC fluxes during 6<sup>th</sup> leaf and silking stages, 45-60 min  
 413 averaging is more appropriate for dough and maturity stages. Similar to carbon and water  
 414 fluxes, the Ogive plots for WUE were presented in Figure 5c. From this, it is observed that the  
 415 flat part of Ogive is achieved at 15 min time average period for the stages of 6<sup>th</sup> leaf and silking  
 416 and 45 min time average for the dough and maturity stages which is similar to the carbon and  
 417 water fluxes. ~~This~~ This concludes that the WUE co-spectrum followed a similar behaviour as its  
 418 individual fluxes i.e. carbon and water fluxes in achieving optimal time averages. The crop  
 419 biophysical factors like LAI and plant height are minimum during 6<sup>th</sup> leaf and silking stages  
 420 contributes low quantity of CO<sub>2</sub> and H<sub>2</sub>O fluxes (refer figure 3a & 3b) whereas they are

421 maximum in the later stages of the crop i.e., dough and maturity contributing to high quantities  
 422 of CO<sub>2</sub> and H<sub>2</sub>O fluxes (refer figure 3a & 3b). Our results are in accordance with the previous  
 423 studies of Fong et al., 2020) on Cotton, where the responses in NPP and ET were related  
 424 seasonally to plant growth stages. The previous studies on various crops revealed that the NPP  
 425 and ET fluxes were initially low in the early stages and increases towards maturity stage due  
 426 to crop phenology and management practices. To capture these low quantity fluxes, low  
 427 averaging periods i.e., 15 min is sufficient, whereas 45 min time-averaging period can capture  
 428 high quantity fluxes that are prevalent during later growth stages of the crop. As the crop  
 429 characteristics are dependent on crop growth stages, a single time-averaging period is not  
 430 appropriate to capture the dynamics of CO<sub>2</sub> and H<sub>2</sub>O fluxes as well their ratio, WUE. This  
 431 clearly demonstrates that, as the plant achieves its higher stage, flux contribution from low-  
 432 frequency components becomes more **valuablepredominant**. Very low averaging periods (ex:  
 433 1 min, 5 min) were found unsuitable to capture low-frequency flux components, which is in  
 434 agreement with literature (Feng, 2017).

435

### 436 3.4 Dynamics of Water use efficiency

437 Daily means of water use efficiency (WUE) estimated with conventional 30 min and  
 438 growth specific optimal averaging periods is presented in Figure 6. Mean WUE fluxes for 6<sup>th</sup>

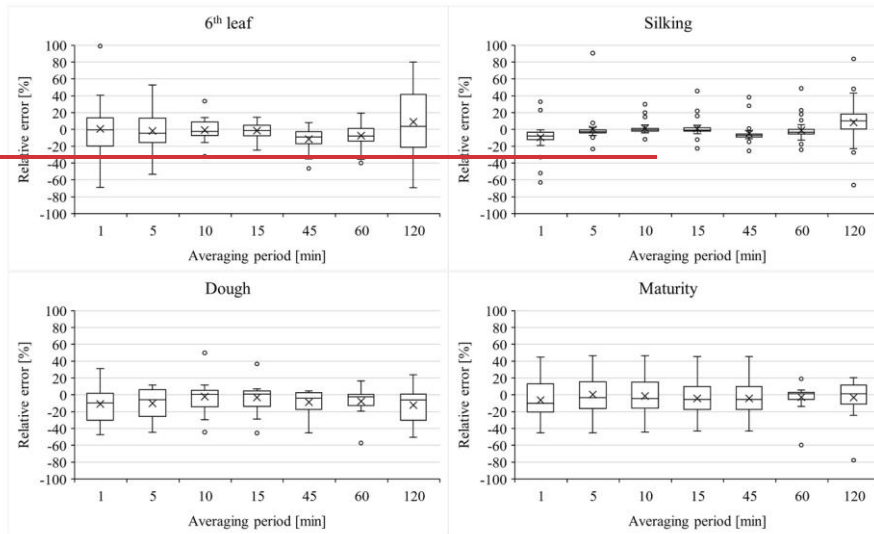


439

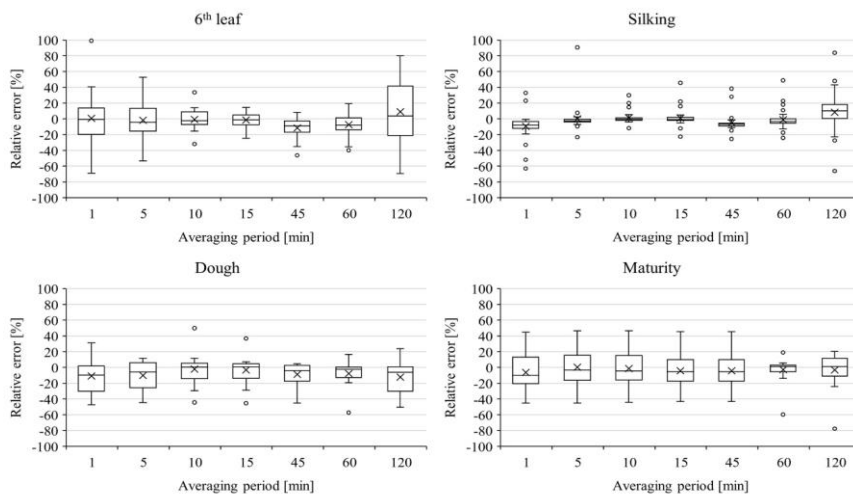
440 **Figure 6:** Seasonal variations in daily mean WUE fluxes obtained with conventional 30 min (solid) and  
 441 optimal averaging periods (dotted) during the crop cycle.

442 leaf, silking, dough and maturity stages with conventional 30 min averaging are  $1.48 \pm 0.96$ ,  
443  $1.36 \pm 0.73$ ,  $1.38 \pm 0.95$  and  $3.184 \pm 0.78$   $\mu\text{mol mmol}^{-1}$  respectively. Corresponding fluxes  
444 with stage specific optimal averaging periods are  $1.49 \pm 0.95$ ,  $1.37 \pm 0.74$ ,  $1.39 \pm 0.79$  and  $3.06$   
445  $\pm 0.69$   $\mu\text{mol mmol}^{-1}$  respectively. Error in estimating mean daily WUE fluxes with 30 min  
446 averaging is very low ( $< 1.45\%$ ) during 6<sup>th</sup> leaf and silking stages, low (8.56 to 9.04 %) during  
447 maturity stage, and is moderate (11.84 to 12.12 %) during dough stage. This conclude that,  
448 choice of optimal averaging period is more crucial for late stage growth periods of the crop.  
449 Distribution of error in estimating WUE fluxes with various averaging periods relative to  
450 conventional 30 min average period (RE) is presented in Figure 7. A close to zero RE with all  
451 averaging periods during 6<sup>th</sup> leaf and silking stages conclude that, choice of averaging period  
452 has insignificant role in estimating the WUE fluxes, particularly during early growth stages. A  
453 slightly high RE ( $\sim -5.4\%$ ) during dough and maturity stages conclude that, choice of averaging  
454 period matters for WUE estimation during late stage periods. Hence, conventional 30 min  
455 averaging period can be considered for estimating WUE fluxes during 6<sup>th</sup> leaf and silking  
456 stages, whereas optimal averaging period need to be considered for estimating WUE fluxes  
457 during dough and maturity stages. Correlation charts showing the linear association  
458 considering within-daily means of carbon, water, and WUE fluxes ~~represented~~ at different  
459 averaging periods is represented in Figure 8. For ease with comparison, data for the entire crop  
460 cycle was considered. Linear association

461



462



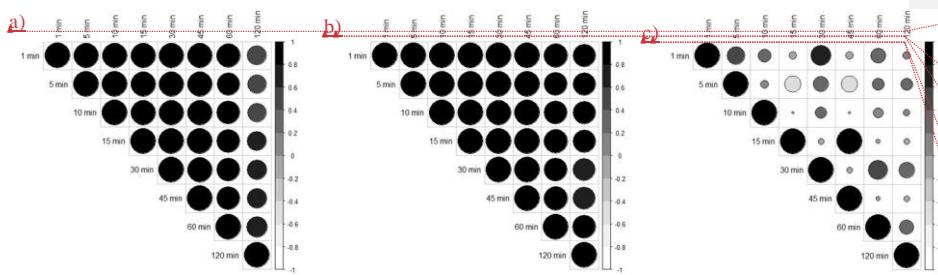
463

464 **Figure 7:** Whisker plots showing the distribution of error in estimating WUE fluxes with various averaging  
 465 periods relative to the conventional 30 min averaging.

466 between any two averaging periods is positive ( $r_p > 0.56$ ) for carbon and water fluxes. Except  
 467 with 120 min time-averaging, all other averaging periods are strongly correlated ( $r_p > 0.87$ )  
 468 with 30 min averaging period. Surprisingly However, a poor linear association in WUE fluxes  
 469 was observed between any two averaging periods, which is attributed to a larger variation in

Formatted: Centered

470 individual WUE fluxes between averaging periods. However, the corresponding individual  
 471 carbon and water fluxes have recorded low variations between time averages. This conclude  
 472 that, the need for optimal averaging period is more crucial in estimating-representing WUE  
 473 fluxes rather than individual carbon and water fluxes. Our findings can improve representation  
 474 of WUE fluxes using EC data, thereby help in developing efficient water management  
 475 strategies in response to WUE changes.



476  
 477 **Figure 8:** Correlation charts showing the linear association of **a)** Carbon fluxes, **b)** Water fluxes, and **c)**  
 478 WUE fluxes estimated with different averaging periods. Circle size represents the correlation magnitude  
 479 and the color sign from white to black represents the negative to positive correlations respectively.

480

#### 481 4.0 CONCLUSIONS

482 This study explores the effect of averaging period of EC fluxes on EBR dynamics and  
 483 WUE in semi-arid Indian conditions. The proposed methodology was applied on drip-irrigated  
 484 Maize field for one crop period (May-Sept 2019). Major findings of this study are:

- 485 • EBR was found to vary marginally at low averaging periods and less significant during  
 486 higher averaging periods.
- 487 • With reference to conventional 30 min averaging period, relative error is within 12%  
 488 for 10-45 min averaging periods for carbon fluxes and is within 5% for 15-45 averaging  
 489 periods for water fluxes.
- 490 • From Ogive analysis we found the optimal averaging period as 15 - 30 min for the 6<sup>th</sup>  
 491 leaf, and silking stages, and as 45 – 60 min for the dough and maturity stages.
- 492 • The mean carbon fluxes are increasing from  $1.81 \pm 0.06 \mu\text{mol}^+1\text{m}^{-2}\text{s}^{-1}$  (6<sup>th</sup> leaf stage) to  
 493  $15.44 \pm 0.75 \mu\text{mol}^+1\text{m}^{-2}\text{s}^{-1}$  (maturity stage) which indicates that carbon sink is a function  
 494 of crop growth period. In case of water fluxes, it increased from  $2.52 \pm 0.13 \text{mmol}^+1\text{m}^{-2}\text{s}^{-1}$

Formatted: Font: (Default) Times New Roman, 10 pt, Font color: Text 1

Formatted: Font: (Default) Times New Roman, 10 pt

Formatted: Font: (Default) Times New Roman, 10 pt, Font color: Text 1

Formatted: Font: (Default) Times New Roman, 10 pt

Formatted: Font: (Default) Times New Roman, 10 pt, Font color: Text 1

Formatted: Superscript

Formatted: Superscript

495  $\mu\text{mol m}^{-2}\text{s}^{-1}$  (6th leaf stage) to  $5.02 \pm 0.29 \text{ mmol}^{+1}\text{m}^{-2}\text{s}^{-1}$  (maturity stage). Variation of carbon  
496 and water fluxes are directly influencing WUE dynamics.

- 497 • The variation in WUE was increased subsequently with the plant growth and achieved  
498 its maximum value of  $5.17 \mu\text{mol mmol}^{-1}$  in between dough to maturity stages which  
499 concludes that, crop consumes more carbon than water as the crop period progresses.
- 500 • The correlation between  $\text{CO}_2$  and  $\text{H}_2\text{O}$  fluxes for all averaging periods was found to be  
501 high. However, WUE, which is calculated as the ratio of  $\text{CO}_2$  and  $\text{H}_2\text{O}$  fluxes, is not  
502 following the same pattern. While 45 min and 15 min averaged WUE exhibits a good  
503 correlation, 30 min averaged WUE is not correlated with other averaging periods.  
504 Averaging period is found to be an influencing factor in controlling WUE, hence should  
505 be considered with caution during the crop growth.

506 This study is limited to understand the role of different time-averaging periods on EC observed  
507 carbon, water fluxes as well as EC derived WUE fluxes contributed by homogeneous Maize  
508 crop which is having relatively smaller flux footprint in an unstable atmospheric condition.  
509 Study findings can help to accurately characterise WUE of Maize crop considering growth  
510 stages for effective implementation of irrigation strategies.

#### 512 Acknowledgments

513 The authors acknowledge the anonymous reviewers for their insightful comments. This  
514 research evolved as an extension of a term project in CE6520-Irrigation Water Management  
515 course at IIT Hyderabad.

#### 517 Data Availability Statement:

518 All footprint climatologies, site-level data files, and supplementary material can be accessed  
519 via the Zenodo Data Repository (<https://zenodo.org/badge/latestdoi/528291820>)  
520 (Shweta07081992, 2022)

#### 522 Author Contribution:

523 **Arun Rao Karimindla:** Data processing and Analysis, Writing- Original draft. **Shweta**  
524 **Kumari:** Conceptualization, Methodology, Project Supervision. **Saipriya SR:** Data processing  
525 Analysis, and Writing- Original draft. **Syam Chintala:** Data processing and Analysis, Writing-



526 Original draft, Reviewing and Editing. BVN Phanindra Kambhammettu: Project  
527 Administration, Writing- Reviewing and Editing.

528

529 **Competing interests:**

530 The authors declare that they have no known competing interests or personal relationships that  
531 could have appeared to influence the work reported in this paper.

532

533 **5.0 REFERENCES**

534 Barr, A. G., Morgenstern, K., Black, T. A., McCaughey, J. H., & Nescic, Z. (2006). Surface  
535 energy balance closure by the eddy-covariance method above three boreal forest stands  
536 and implications for the measurement of the CO<sub>2</sub> flux. *Agricultural and Forest*  
537 *Meteorology*, 140(1–4), 322–337. <https://doi.org/10.1016/j.agrformet.2006.08.007>

538 Bramley, H., Turner, N. C., & Siddique, K. H. M. (2013). Water Use Efficiency. In C. Kole  
539 (Ed.), *Genomics and Breeding for Climate-Resilient Crops: Vol. 2 Target Traits* (pp.  
540 225–268). Springer Berlin Heidelberg. [https://doi.org/10.1007/978-3-642-37048-9\\_6](https://doi.org/10.1007/978-3-642-37048-9_6)

541 Berger, B. W., Davis, K. J., Yi, C., Bakwin, P. S., & Zhao, C. L. (2001). Long-term carbon  
542 dioxide fluxes from a very tall tower in a northern forest: Flux measurement  
543 methodology. *Journal of Atmospheric and Oceanic Technology*, 18(4), 529–542.

544 Central Ground Water Board. (2015). Annual Report 2013.

545 [https://cgwb.gov.in/old\\_website/Annual-Reports/Annual-Report-2013-14.pdf](https://cgwb.gov.in/old_website/Annual-Reports/Annual-Report-2013-14.pdf)

546 Charuchittipan, D., W. Babel, M. Mauder, J. P. Leps, and T. Foken, 2014: Extension of the  
547 Averaging Time in Eddy-Covariance Measurements and Its Effect on the Energy  
548 Balance Closure. *Boundary-Layer Meteorol.*, **152**, 303–327,  
549 <https://doi.org/10.1007/s10546-014-9922-6>.

550 Chen, Y. Y., and M. H. Li, 2012: Determining adequate averaging periods and reference  
551 coordinates for eddy covariance measurements of surface heat and water vapor fluxes  
552 over mountainous terrain. *Terr. Atmos. Ocean. Sci.*, **23**, 685–701,  
553 [https://doi.org/10.3319/TAO.2012.05.02.01\(Hy\)](https://doi.org/10.3319/TAO.2012.05.02.01(Hy)).

554 Chintala, S., Karimindla, A. R., & Kambhammettu, B. V. N. P. (2024). Scaling relations  
555 between leaf and plant water use efficiencies in rainfed Cotton. *Agricultural Water*

- 556 Management, 292, 108680. <https://doi.org/https://doi.org/10.1016/j.agwat.2024.108680>
- 557 Desjardins, R. L., MacPherson, J. I., Schuepp, P. H., & Karanja, F. (1989). An evaluation of  
558 aircraft flux measurements of CO<sub>2</sub>, water vapor and sensible heat. *Boundary-Layer*  
559 *Meteorology*, 47(1), 55–69. <https://doi.org/10.1007/BF00122322>
- 560 Eshonkulov, R., and Coauthors, 2019: Evaluating multi-year, multi-site data on the energy  
561 balance closure of eddy-covariance flux measurements at cropland sites in southwestern  
562 Germany. *Biogeosciences*, **16**, 521–540, <https://doi.org/10.5194/bg-16-521-2019>.
- 563 Feng, J., B. Zhang, Z. Wei, and D. Xu, 2017: Effects of Averaging Period on Energy Fluxes  
564 and the Energy-Balance Ratio as Measured with an Eddy-Covariance System.  
565 *Boundary-Layer Meteorol.*, **165**, 545–551, <https://doi.org/10.1007/s10546-017-0284-8>.
- 566 Ficci, 2014: Maize in India. *India Maize Summit '14*, 1–32.
- 567 Finkelstein, P. L., & Sims, P. F. (2001). Sampling error in eddy correlation flux  
568 measurements. *Journal of Geophysical Research*, 106, 3503–3509.  
569 <https://api.semanticscholar.org/CorpusID:128980052>
- 570 Finnigan, J. J., 2004: A re-evaluation of long-term flux measurement techniques part II:  
571 Coordinate systems. *Boundary-Layer Meteorol.*, **113**, 1–41,  
572 <https://doi.org/10.1023/B:BOUN.0000037348.64252.45>.
- 573 Finnigan, J. J., R. Clement, Y. Malhi, R. Leuning, and H. A. Cleugh, 2003: Re-evaluation of  
574 long-term flux measurement techniques. Part I: Averaging and coordinate rotation.  
575 *Boundary-Layer Meteorol.*, **107**, 1–48, <https://doi.org/10.1023/A:1021554900225>.
- 576 Foken, T., and B. Wichura, 1996: Tools for quality assessment of surface-based flux  
577 measurements. *Agric. For. Meteorol.*, **78**, 83–105, [https://doi.org/10.1016/0168-](https://doi.org/10.1016/0168-1923(95)02248-1)  
578 [1923\(95\)02248-1](https://doi.org/10.1016/0168-1923(95)02248-1).
- 579 Foken, T., Göockede, M., Mauder, M., Mahrt, L., Amiro, B., & Munger, W. (2005). Post-  
580 Field Data Quality Control BT - Handbook of Micrometeorology: A Guide for Surface  
581 Flux Measurement and Analysis (X. Lee, W. Massman, & B. Law, Eds.; pp. 181–208).  
582 Springer Netherlands. [https://doi.org/10.1007/1-4020-2265-4\\_9](https://doi.org/10.1007/1-4020-2265-4_9)
- 583 Foken, T., M. Aubinet, J. J. Finnigan, M. Y. Leclerc, M. Mauder, and K. T. Paw U, 2011:  
584 Results of a panel discussion about the energy balance closure correction for trace gases.  
585 *Bull. Am. Meteorol. Soc.*, **92**, <https://doi.org/10.1175/2011BAMS3130.1>.

- 586 Fong, B. N., Reba, M. L., Teague, T. G., Runkle, B. R. K., & Suvočarev, K. (2020). Eddy  
 587 covariance measurements of carbon dioxide and water fluxes in US mid-south cotton  
 588 production. *Agriculture, Ecosystems and Environment*, 292.  
 589 <https://doi.org/10.1016/j.agee.2019.106813>
- 590 Gao, Z., H. Liu, G. G. Katul, and T. Foken, 2017: Non-closure of the surface energy balance  
 591 explained by phase difference between vertical velocity and scalars of large atmospheric  
 592 eddies. *Environ. Res. Lett.*, **12**, <https://doi.org/10.1088/1748-9326/aa625b>.
- 593 [Guo, H., Li, S., Wong, F. L., Qin, S., Wang, Y., Yang, D., & Lam, H. M. \(2021\). Drivers of](#)  
 594 [carbon flux in drip irrigation maize fields in northwest China. \*Carbon Balance and\*](#)  
 595 [\*Management\*, 16\(1\), 1–16. <https://doi.org/10.1186/s13021-021-00176-5>](#)
- 596 Gerken, T., and Coauthors, 2018: Investigating the mechanisms responsible for the lack of  
 597 surface energy balance closure in a central Amazonian tropical rainforest. *Agric. For.*  
 598 *Meteorol.*, **255**, 92–103, <https://doi.org/10.1016/j.agrformet.2017.03.023>.
- 599 Kidston, J., Brümmer, C., Black, T. A., Morgenstern, K., Nesic, Z., McCaughey, J. H., &  
 600 Barr, A. G. (2010). Energy balance closure using eddy covariance above two different  
 601 land surfaces and implications for CO<sub>2</sub> flux measurements. *Boundary-Layer*  
 602 *Meteorology*, 136(2), 193–218. <https://doi.org/10.1007/s10546-010-9507-y>
- 603 Kole, C., 2013: *Genomics and breeding for climate-resilient crops: Vol. 2 target traits*. 1–474  
 604 pp.
- 605 Kottek, M., J. Grieser, C. Beck, B. Rudolf, and F. Rubel, 2006: World map of the Köppen-  
 606 Geiger climate classification updated. *Meteorol. Zeitschrift*, **15**, 259–263,  
 607 <https://doi.org/10.1127/0941-2948/2006/0130>.
- 608 Leclerc, M. Y., and T. Foken, 2014: *Footprints in micrometeorology and ecology*. Springer,.
- 609 Lee, X., Q. Yu, X. Sun, J. Liu, Q. Min, Y. Liu, and X. Zhang, 2004: Micrometeorological  
 610 fluxes under the influence of regional and local advection: A revisit. *Agric. For.*  
 611 *Meteorol.*, **122**, 111–124, <https://doi.org/10.1016/j.agrformet.2003.02.001>.
- 612 Leuning, R., E. van Gorsel, W. J. Massman, and P. R. Isaac, 2012: Reflections on the surface  
 613 energy imbalance problem. *Agric. For. Meteorol.*, **156**, 65–74,  
 614 <https://doi.org/10.1016/j.agrformet.2011.12.002>.
- 615 Malhi, Y., K. McNaughton, and C. Von Randow, 2004: Low Frequency Atmospheric

Formatted: Justified

616 Transport and Surface Flux Measurements. 101–118, [https://doi.org/10.1007/1-4020-](https://doi.org/10.1007/1-4020-2265-4_5)  
617 2265-4\_5.

618 Manon, M., and M. Kristian, 2020: Estimating local atmosphere-surface fluxes using eddy  
619 covariance and numerical Ogive optimization. **15**, 21387–21432,  
620 <https://doi.org/10.5194/acpd-14-21387-2014>.

621 Mauder, M., and T. Foken, 2006: Impact of post-field data processing on eddy covariance  
622 flux estimates and energy balance closure. *Meteorol. Zeitschrift*, **15**, 597–609,  
623 <https://doi.org/10.1127/0941-2948/2006/0167>.

624 Medrano, H., and Coauthors, 2015: From leaf to whole-plant water use efficiency (WUE) in  
625 complex canopies: Limitations of leaf WUE as a selection target. *Crop J.*, **3**, 220–228,  
626 <https://doi.org/10.1016/j.cj.2015.04.002>.

627 Meyers, T. P., & Hollinger, S. E. (2004). An assessment of storage terms in the surface energy  
628 balance of maize and soybean. *Agricultural and Forest Meteorology*, 125(1–2), 105–115.  
629 <https://doi.org/10.1016/j.agrformet.2004.03.001>

Formatted: Justified

630 Oncley, S. P., and Coauthors, 2007: The energy balance experiment EBEX-2000. Part I:  
631 Overview and energy balance. *Boundary-Layer Meteorol.*, **123**, 1–28,  
632 <https://doi.org/10.1007/s10546-007-9161-1>.

633 Peddinti, S. R., and B. P. Kambhammettu, 2019: Dynamics of crop coefficients for citrus  
634 orchards of central India using water balance and eddy covariance flux partition  
635 techniques. *Agric. Water Manag.*, 212, 68–77,  
636 <https://doi.org/10.1016/j.agwat.2018.08.027>

637 Peddinti, S. R., Kambhammettu, B. V. N. P., Rodda, S. R., Thumaty, K. C., & Suradhaniwar,  
638 S. (2020). Dynamics of Ecosystem Water Use Efficiency in Citrus Orchards of Central  
639 India Using Eddy Covariance and Landsat Measurements. *Ecosystems*, 23(3), 511–528.  
640 <https://doi.org/10.1007/s10021-019-00416-3>

641 Rahman, M. M., Zhang, W., & Wang, K. (2019). Assessment on surface energy imbalance and  
642 energy partitioning using ground and satellite data over a semi-arid agricultural region in  
643 north China. *Agricultural Water Management*, 213(June 2018), 245–259.  
644 <https://doi.org/10.1016/j.agwat.2018.10.032>

Formatted: Justified

645 Reed, D. E., J. M. Frank, B. E. Ewers, and A. R. Desai, 2018: Time dependency of eddy

- 646 covariance site energy balance. *Agric. For. Meteorol.*, **249**, 467–478,  
647 <https://doi.org/10.1016/j.agrformet.2017.08.008>.
- 648 Sakai, R. K., D. R. Fitzjarrald, and K. E. Moore, 2001: Importance of low-frequency  
649 contributions to eddy fluxes observed over rough surfaces. *J. Appl. Meteorol.*, **40**, 2178–  
650 2192, [https://doi.org/10.1175/1520-0450\(2001\)040<2178:IOLFCT>2.0.CO;2](https://doi.org/10.1175/1520-0450(2001)040<2178:IOLFCT>2.0.CO;2).
- 651 Sharma, B. R., Gulati, Mohan, Gayathri, Manchanda, S., Ray, I., & Amarasinghe, U. (2018).  
652 Water Productivity Mapping of Major Indian Crops. NABARD and ICRIER, 4(1), 88–  
653 100.
- 654 Shankar, V., C. S. P. Ojha, and K. S. H. Prasad, 2012: Irrigation Scheduling for Maize and  
655 Indian-mustard based on Daily Crop Water Requirement in a Semi- Arid Region. **6**,  
656 476–485.
- 657 Soujanya, B., B. B. Naik, M. U. Devi, T. L. Neelima, and A. Biswal, 2021: Dry Matter  
658 Production and Nitrogen Uptake as Influenced by Irrigation and Nitrogen Levels in  
659 Maize. *Int. J. Environ. Clim. Chang.*, 155–161,  
660 <https://doi.org/10.9734/ijecc/2021/v11i1130528>.
- 661 Sun, X. M., Z. L. Zhu, X. F. Wen, G. F. Yuan, and G. R. Yu, 2006: The impact of averaging  
662 period on eddy fluxes observed at ChinaFLUX sites. *Agric. For. Meteorol.*, **137**, 188–  
663 193, <https://doi.org/10.1016/j.agrformet.2006.02.012>.
- 664 Tang, X., Z. Ding, H. Li, X. Li, J. Luo, J. Xie, and D. Chen, 2015: Characterizing ecosystem  
665 water-use efficiency of croplands with eddy covariance measurements and MODIS  
666 products. *Ecol. Eng.*, **85**, 212–217, <https://doi.org/10.1016/j.ecoleng.2015.09.078>.
- 667 Tong, X., J. Zhang, P. Meng, J. Li, and N. Zheng, 2014: Ecosystem water use efficiency in a  
668 warm-temperate mixed plantation in the North China. *J. Hydrol.*, **512**, 221–228,  
669 <https://doi.org/10.1016/j.jhydrol.2014.02.042>.
- 670 Tong, X. J., J. Li, Q. Yu, and Z. Qin, 2009: Ecosystem water use efficiency in an irrigated  
671 cropland in the North China Plain. *J. Hydrol.*, **374**, 329–337,  
672 <https://doi.org/10.1016/j.jhydrol.2009.06.030>.
- 673 Twine, T. E., and Coauthors, 2000: Correcting eddy-covariance flux underestimates over a  
674 grassland. *Agric. For. Meteorol.*, **103**, 279–300, [https://doi.org/10.1016/S0168-](https://doi.org/10.1016/S0168-1923(00)00123-4)  
675 [1923\(00\)00123-4](https://doi.org/10.1016/S0168-1923(00)00123-4).

- 676 Vickers, D., & Mahrt, L. (1997). Quality control and flux sampling problems for tower and  
677 aircraft data. *Journal of Atmospheric and Oceanic Technology*, 14(3), 512–526.  
678 [https://doi.org/10.1175/1520-0426\(1997\)014<0512:QCAFSP>2.0.CO;2](https://doi.org/10.1175/1520-0426(1997)014<0512:QCAFSP>2.0.CO;2)
- 679 Wang, X., C. Wang, and B. Bond-Lamberty, 2017: Quantifying and reducing the differences  
680 in forest CO<sub>2</sub>-fluxes estimated by eddy covariance, biometric and chamber methods: A  
681 global synthesis. *Agric. For. Meteorol.*, **247**, 93–103,  
682 <https://doi.org/10.1016/j.agrformet.2017.07.023>.
- 683 Wilson, K., E. Falge, M. Aubinet, and D. Baldocchi, 2002: DigitalCommons @ University of  
684 Nebraska - Lincoln Energy Balance Closure at FLUXNET Sites. *Agric. For. Meteorol.*,  
685 223–243.
- 686 Zhang, P., G. Yuan, and Z. Zhu, 2013: Determination of the averaging period of eddy  
687 covariance measurement and its influences on the calculation of fluxes in desert riparian  
688 forest. *Arid L. Geogr.*, **36**, 401–407.
- 689
- 690